RSC Advances

ROYAL SOCIETY OF CHEMISTRY

www.rsc.org/advances

ARTICLE TYPE www. rsc.org/xxxxxx | XXXXXXXX

Imaging and spectroscopy of Au nanoclusters in yttria stabilized zirconia films by Ballistic Electron/Hole Emission Microscopy

Dmitry Filatov,*[a] Davud Guseinov,[b] Ivan Antonov,[b] Alexander Kasatkin,[b] and Oleg Gorshkov[a,b]

Received Xth XXXXXXXXXX 20XX, Accepted Xth XXXXXXXXX 20XX
First published on the web Xth XXXXXXXXXX 200X
DOI: 10.1039/b000000x

Ballistic Electron/Hole Emission Microscopy (BEEM/BHEM) has been applied to imaging and spectroscopy of Au nanoclusters (NCs) embedded into the ultrathin (≈ 6 nm thick) yttria stabilized zirconia (YSZ) films on Si substrates prepared by Magnetron Sputtering and annealing. Such structures are promising for the resistive switching non-volatile memory applications. According to the High Resolution Cross-sectional Transmission Electron Microscopy (HR X-TEM) data, the nearly spherical Au NCs of 1.5 to 3.5 nm in diameter were arranged almost in a single sheet between the YSZ layers. The BEEM images demonstrated the spots of increased collector current of 1 to 2.5 nm in size related to the ballistic electron tunnelling via the Au NCs. BEEM/BHEM spectra of the NCs demonstrated the stepwise features attributed to the quantum confined states in the Au NCs. The estimate of the NC diameter by the best fit between the quantum confined state energies determined from the BEEM/BHEM spectra and the ones calculated for a spherical quantum dot yielded 1.7 to 3.3 nm that is consistent with the HR X-TEM data. The results of present study demonstrate the capabilities of BEEM/BHEM in characterization of the ultrathin dielectric films with metal NCs in research and also in production.

1 Introduction

Recently, the metal nanoclusters (NCs) embedded into the ultrathin (∼ 10 nm thick) dielectric films attracted much attention because of their potential application in the floating gate Metal-Oxide-Semiconductor Field Effect Transistors (MOSFETs), which are promising for the non-volatile memory devices[1]. The NC structure and size control as well as the electronic structure are essential in their device applications. Transmission Electron Microscopy (TEM) is applied for structural characterization of the metal NCs in the dielectric matrices widely[2]. As for the electronic structure of the metal NCs, until recently there were no experimental techniques for direct measurements of the electron size quantization spectra in the NCs in the dielectrics. Generally, the experimental observation of the quantum size effects in the metal NCs are very complicated due to the scatter of NCs' sizes and shapes[3]. Scanning Tunnelling Microscopy (STM) allows direct measurements of the electron energy spectra in the individual supported NCs[4]. However, the STM investigations of the NCs in the dielectric matrices meet serious problems. In order to maintain a stable STM feedback, the nanocomposite films should possess a considerable conductivity either via the tunnel mechanism or via the percolation one[5,6]. The former imposes strict limitations on the dielectric thickness and hence, on the NCs sizes while the latter requires a high volume density of the NCs inside the dielectric that makes the tunnel spectroscopy of the individual NCs impossible.

Earlier, we have applied Tunnelling Atomic Force Microscopy (AFM) to imaging and tunnel spectroscopy of individual Au NCs inside the ultrathin (4 to 5 nm thick) SiO_2/Si(001) films prepared by Pulsed Laser Deposition (PLD)[7]. The Au NCs manifested themselves as the spots of increased tip current I_t attributed to the electron tunnelling between the AFM tip and the n^+-Si substrate via individual Au NCs. The peaks attributed to the electron tunnelling via the quantum confined states in the ultrafine (∼ 1 nm in size) Au NCs have been observed in the tunnel spectra of the SiO_2:nc-Au/Si films. We attempted to extract the size quantization spectra in the Au NCs by the best fit between the model tunnel spectra and the measured ones[8]. However, this approach was neither much informative nor reliable.

In the present study, we have applied Ballistic Electron/Hole Emission Microscopy (BEEM/BHEM) to imaging and tunnel spectroscopy of the quantum confined electron states in the Au NCs in the ultrathin (≈ 6 nm) yttria stabilized zirconia (YSZ) films on Si. Such films are promising

* *Corresponding author. Research and Educational Center for Physics of Solid State Nanostructures, Lobachevskii State University of Nizhni Novgorod, 23 Gagarin Ave. Building 3, Nizhni Novgorod, Russian Federation. Fax: +7 831 462 3136; Tel: +7 910 797 9536; E-mail: dmitry_filatov@inbox.ru*
[a] *Research and Educational Center for Physics of Solid State Nanostructures, Lobachevskii State University of Nizhni Novgorod, 23 Gagarin Ave. Building 3, Nizhni Novgorod, Russian Federation.*
[b] *Physical-Technical Research Institute, Lobachevskii State University of Nizhni Novgorod, 23 Gagarin Ave. Building 3, Nizhni Novgorod, Russian Federation.*

for the resistive non-volatile memory applications[9]. Earlier, BEEM/BHEM has been proven to be a powerful tool for measuring the energy barriers in the MOS stacks as well as for imaging and spectroscopy of the semiconductor quantum dots (QDs)[10]. The aim of the present work was to investigate the capabilities of BEEM/BHEM in imaging the metal NCs in the ultrathin dielectric films as well as in a direct measurement of the quantum confined state energies in the metal NCs.

2 Experimental

The YSZ films were deposited by Radio Frequency Magnetron Sputtering (the oscillator frequency was ≈ 13.56 MHz) at the substrate temperature $(300 \pm 10)^{\circ}$C using Torr International 2G1-1G2-eb4-th1 vacuum setup for thin film deposition from a sintered powder target made from $ZrO_2 - Y_2O_3$ powders mixture. The initial powders were of chemical purity (the impurity molar fraction was $< 10^{-3}$). The molar fraction of Y_2O_3 was 0.12 ± 0.01.

The nanocomposite YSZ:nc-Au/Si films for BEEM/BHEM investigations were prepared by the deposition of the three-layered stacks consisted of the (3.0 ± 0.5) nm thick underlying YSZ layers, the Au layers with the nominal thickness of (1.0 ± 0.1) nm, and the (3.0 ± 0.5) nm thick cladding YSZ layers onto the *n*-Si(001) substrates followed by annealing. Also, the YSZ/Si(001) films of (6.0 ± 0.2) nm in thickness were fabricated to serve as the reference samples. The Si Epiready-grade polished (the surface roughness was < 0.2 nm) substrates of the semiconductor grade purity with the electron concentration $n = (2.5 \pm 0.5) \times 10^{15}$ cm^{-3} were used. The Au layers were deposited from a metal target made of pure Au (the impurity molar fraction was $< 10^{-4}$). The deposition process was carried out in the mixture of Ar and O_2 (50 : 50 % mol.), both gases were of high purity (the impurity molar fraction was $< 5 \times 10^{-6}$). The gas pressure inside the deposition chamber was $(1.0 \pm 0.1) \times 10^{-2}$ Torr. The stacks were annealed in air at $(800 \pm 15)^{\circ}$C for (2.00 ± 0.03) min. Finally, the Au base electrodes of (5.0 ± 0.5) nm in thickness were deposited onto the YSZ surfaces.

The BEEM/BHEM experiments were carried out in ambient air at room temperature using a home-made setup based on NT-MDT Solver Pro scanning probe microscope (SPM). The scanning sample scheme was utilized. The first stage collector current preamplifier (the current voltage converter) was built inside the sample holder mounted onto the tube piezoscanner. The ground contacts to the Au base electrodes were provided by a bronze spring. The home-made STM head utilized a tip-biased tip current preamplifier form NT-MDT Smena EC electrochemical SPM head. The STM probes were made from a W wire (technical purity grade, the impurity molar fraction $< 10^{-2}$) sharpened by electrochemical etching in a 0.5M solution of NaOH (chemical purity grade, the impurity molar fraction $< 10^{-3}$) in distilled deionized water (the specific resistivity $> 10^{11}$ $\Omega \times$cm).

The BEEM/BHEM images were recorded in the constant current mode. The BEEM/BHEM spectra were measured with the tip current feedback switched on. The uncertainties of the primary measurements of the gap voltage V_g (applied between the STM tip and the Au base) and of the collector current I_c were 1 mV and 2 pA, respectively. The differential BEEM/BHEM spectra dI_c/dV_g were calculated from the measured $I_c(V_g)$ curves by numerical differentiation with nonlinear smoothing. More details on the apparatus design as well as on the measurements procedures can be found elsewhere[11].

3 Results and discussion

3.1 YSZ films on Si substrates

The cyclic BEEM spectra of an Au(5 nm)/YSZ(6 nm)/*n*-Si reference sample (Fig. 1) demonstrated a well expressed hysteresis. The spectra were measured in the Ballistic Electron Emission Spectroscopy (BEES) mode. The gap voltage V_g was swept forward from 0 V downto -3 V and backward from -3 V up to 0 V. The curves measured at the forward V_g sweep demonstrated the thresholds at $V_g = (-2.5 \pm 0.1)$ V related to the YSZ conduction band edge E_c (Fig. 2). Also, the peaks at $V_t = (-2.2 \pm 0.1)$ V attributed to the electron transport via the oxygen vacancy band (α-band) in YSZ[12] with the energy $\approx E_c - 0.3$ eV have been observed. The hysteresis in the BEEM spectra was attributed to the damage of the sample by the increased setpoint tip current $I_t = 10$ nA at $V_g < -2.5$ V so that a pinhole has been burned through both the Au base and the YSZ layer. The BEES measurements in a pinhole appeared to be a powerful tool for the investigations of the inner barriers in the complex structures[13]. In the present study, the thresholds at $V_g = (-0.5 \pm 0.1)$ V have been observed in the curves recorded at the backward V_g sweep (Fig. 1). These thresholds were related to the conduction band edge in the Si substrate at the YSZ/Si interface $E_{c\mathrm{Si}}$ (Fig. 2). Because of relatively small sizes of the pinhole (several nanometers) the surface potential at the Si surface inside the pinhole could be assumed to be equal to the one at the YSZ/Si interface outside the hole[13]. The conduction band edge in the quasi neutral layer of the Si substrate $E_{c\mathrm{Si0}}$ relative to the Fermi level energy E_F for non-degenerated *n*-Si could be calculated according to a well known formula[14]

$$E_{c\mathrm{Si0}} - E_F = \frac{kT}{e} \ln\left(\frac{N_c}{n}\right) \qquad (1)$$

where k is Boltzmann constant, T is the temperature, e is the elementary charge, and N_c is the effective density of states in the conduction band of Si. For $n = 2.5 \times 10^{15}$ cm^{-3} at 300K one gets $E_{c\mathrm{Si0}} - E_F \approx 0.25$ eV. So far, the potential barrier

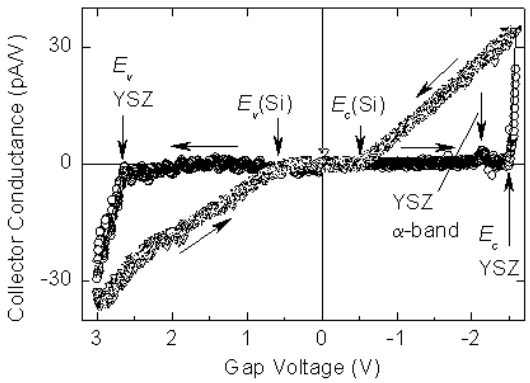

Fig. 1 The cyclic BEEM and BHEM spectra (300K) of an Au(5 nm)/YSZ(6 nm)/*n*-Si stack measured in different points of the sample surface at the setpoint tip current $I_t = 10$ nA. The directions of the gap voltage V_g sweep are marked by the arrows.

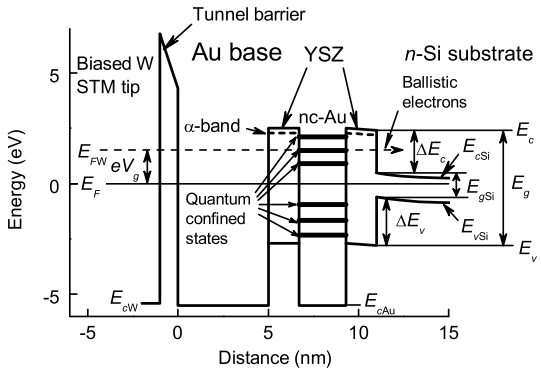

Fig. 2 Band diagram of a contact of a STM tip to an Au(5 nm)/YSZ(3 nm)/nc-Au/YSZ(3 nm)/*n*-Si stack calculated from the BEES/BHES data and the schematic representation of the ballistic electron transport via a quantum confined state in the Au NC in the BEES measurements.

height at the YSZ/Si interface $\Delta\varphi = E_{c\mathrm{Si}} - E_{c\mathrm{Si}0} \approx 0.25$ eV. Now, the conduction band offset at the YSZ/Si interface can be found taking into account the potential drop across the YSZ film from the condition of the electric flux density continuity at the YSZ/Si interface:

$$\varepsilon_{\mathrm{YSZ}} F_{\mathrm{YSZ}} = \varepsilon_{\mathrm{Si}} F_{\mathrm{Si}} \qquad (2)$$

where F_{YSZ} and $\varepsilon_{\mathrm{YSZ}}$ are the electric field strength and the dielectric constant for YSZ, respectively; F_{Si} and $\varepsilon_{\mathrm{Si}}$ are the respective quantities for Si. Assuming $(\varepsilon_{\mathrm{YSZ}} = 25)$[12] and $(\varepsilon_{\mathrm{Si}} = 11.7)$[14] one gets $\Delta E_c = (1.9 \pm 0.1)$ eV. This value is greater than the one calculated theoretically for ZrO_2 (1.4 eV)[15]. However, it is well known that the actual values of the band offsets at the oxide/semiconductor interfaces measured experimentally differ from the theoretical ones often[16]. On the other hand, the values of the YSZ/Si band offsets may differ from the ones for ZrO_2/Si due to a considerable fraction of Y in the films studied in the present work (the respective values for Y_2O_3/Si interface are $\Delta E_c = 2.3$ eV and $\Delta E_v = 2.6$ eV)[16]. However, the quantitative analysis of this effect is difficult because the band offsets in YSZ may vary with the Y fraction nonlinearly. All the above makes the band offset data obtained experimentally (e. g. by BEES) especially valuable.

A hysteresis has also been observed in the spectra recorded at the positive tip bias with respect to the Au base, *i. e.* in the Ballistic Hole Emission Spectroscopy (BHES) mode (Fig. 1). The gap voltage V_g was swept forward from 0 V up to 3 V and backward from 3 V downto 0 V. Note that the cyclic BEEM and BHEM spectra presented in Fig. 1 were measured in different points of the sample surface. Once a pinhole was made in the YSZ film, the thresholds related to the band edges in the Si substrates could be observed only[13].

The thresholds at $V_g = (2.7 \pm 0.1)$ V in the BHEM spectra measured at the forward V_g sweep have been attributed to the YSZ valence band edge E_v (Fig. 2). Note that according to this result, the Fermi energy in Au base ($E_F - E_{c\mathrm{Au}} \approx 5.5$ eV)[17] is higher than the energy spacing between the Fermi level in the Au base E_F and the valence band edge in YSZ $E_F - E_v \approx 2.7$ eV (see Fig. 2). This factor makes the observation of the threshold related to the YSZ valence band edge in the BHEM spectra possible. The threshold at $V_g = (0.6 \pm 0.1)$ V observed at the backward V_g sweep was related to the valence band edge in Si at the YSZ/Si interface $E_{v\mathrm{Si}}$. From the above data, one can calculate the valence band offset at the YSZ/Si interface $\Delta E_v = (2.1 \pm 0.1)$ eV. Again, this value appears to be less than the theoretical one for ZrO_2 (3.3 eV)[15] that is also not surprising taking into account all the above. Note that the resulting energy gap for Si $E_{g\mathrm{Si}} = 0.5$ eV $+0.6$ eV $= 1.1$ eV is consistent with the reference data[14] that confirms the accuracy of the BEES/BHES measurements.

On the other hand, these measurements yielded the YSZ energy gap $E_g = (5.2 \pm 0.1)$ eV, which appears to be less than the respective value obtained for the YSZ films with close Y molar fraction by optical transmission spectroscopy [(5.6 ± 0.1) eV at 300K][18]. This disagreement could probably be attributed to the residual strain in the YSZ film originating from the difference in the thermal expansion coefficients for Si and YSZ [$(\approx 2.6 \times 10^{-6}\ \mathrm{K}^{-1})$[14] and $(\approx 8 \times 10^{-6}\ \mathrm{K}^{-1})$[12], respectively]. On the other hand, the results of the High Resolution Cross-sectional TEM (HR X-TEM) analysis of the YSZ:nc-Au/Si nanocomposite films prepared in the same setup in similar conditions[19] revealed a nanocrystalline structure of YSZ after annealing (the nanocrystal sizes were comparable to the YSZ

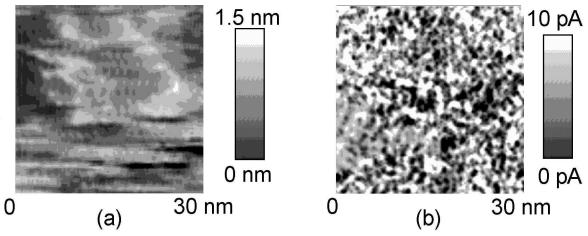

Fig. 3 STM topography (a) and BEEM (b) images of an Au(5 nm)/YSZ(3 nm)/nc-Au/YSZ(3 nm)/*n*-Si stack measured at the setpoint tip current $I_t = 10$ nA and the gap voltage $V_g = -2$ V. The NC, which the BEEM/BHEM spectrum shown in Fig. 4 was measured in is marked by a circle an an arrow.

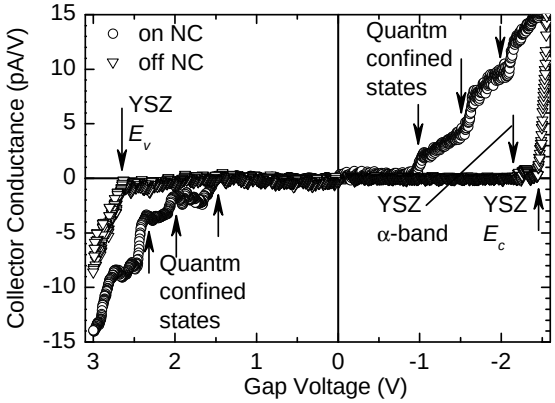

Fig. 4 The BEEM and BHEM spectra (300K) measured on an Au(5 nm)/YSZ(3 nm)/nc-Au/YSZ(3 nm)/*n*-Si stack at the setpoint tip current $I_t = 2$ nA. The NC, which the BEEM and BHEM spectra were measured in is marked by a circle and an arrow in Fig. 3. The arrows mark the quantum confined states in the Au NC.

film thickness). This could be another possible reason for the disagreement of the band gap value for YSZ/Si obtained in the present work with the data reported in the literature[18].

Thus, applying the combination of BEES and BHES allowed measuring all energy gaps in Au/YSZ/Si MOS stack necessary to calculate a complete band diagram of the structure shown in Fig. 2. These energy gaps obtained have been used further to calculate the quantum confined level energies in the Au NCs in the YSZ matrix.

3.2 YSZ films with Au nanoclusters

The STM image of the Au(5 nm)/YSZ(3 nm)/nc-Au/YSZ(3 nm)/*n*-Si stack [Fig. 3(a)] demonstrated an islanded surface typical for thin Au films deposited by Magnetron Sputtering. At the same time, the BEEM image of this sample [Fig. 3(b)] recorded simultaneously with the STM one demonstrated the spots of increased collector current I_c of 1.7 ± 0.6 nm in size related to the ballistic electron tunnelling via the Au NCs, as shown in Fig. 2. The HR X-TEM studies of the YSZ:nc-Au/Si stacks prepared in the similar conditions[19] revealed nearly spherical Au NCs with the diameter $D_c = (2.5 \pm 1.0)$ nm to be arranged in a single sheet between the YSZ layers almost strictly. The surface density of the spots in the BEEM image in Fig. 3(b) $N_s = (3.4 \pm 0.3) \times 10^{13}$ cm^{-2} is of the same order of magnitude as the NC density estimated from the TEM data ($\sim 10^{13}$ cm^{-2})[19] that could be treated as an evidence for the relation of the spots of the increased I_c in the BEEM image to the ballistic electron tunnelling via the Au NCs. Note that there is almost no correlation between the STM and BEEM images in Figures 3(a) and 3(b), respectively except the variations of the averaged BEEM image brightness [Fig. 3(b)] in the scales of ~ 10 nm, which is of the same order of magnitude to the typical sizes of the Au grains in the STM image [Fig. 3(a)]: namely, the higher the local thickness of the Au film, the darker the background of the BEEM image. This artifact is typical for the BEEM investigations[10] and is related to a higher total electron energy loss in a thicker metal base film.

On the other hand, no topographic features corresponding to the smaller sized (1 to 3 nm) bright spots in the BEEM image [Fig. 3(b)] have been observed in the STM image [Fig. 3(a)]. This fact could be treated as another evidence for the relation of the relation of the spots of increased I_c in Fig. 3(b) to the ballistic electron tunnelling via the Au NCs.

Typically, the effective electron probe diameter in BEEM, which, in turn, determine the spatial resolution of the method could be estimated to be (≈ 1 nm)[10] that is less then the typical NC diameter in the structures studied in the present work. So far, BEEM allows the ballistic electron spectroscopy of the individual NCs. Typical BEEM spectra dI_c/dV_g of the Au(5 nm)/YSZ(3 nm)/nc-Au/YSZ(3 nm)/*n*-Si stack are presented in Fig. 4. The BEEM spectra measured between the Au NCs exhibited the thresholds at $V_g = (-2.4 \pm 0.1)$ V and the peaks at $V_g = (-2.1 \pm 0.1)$ V (Fig. 4) attributed to the conduction band edge in YSZ E_c and to the oxygen vacancy α-band in YSZ, respectively, as in the BEEM spectra of the reference Au(5 nm)/YSZ(6 nm)/*n*-Si stack (Fig. 1). The BEEM spectra measured recorded in the spots of increased I_c (corresponding to the Au NCs) demonstrated the stepwise features attributed to the quantum confined states in the Au NCs. The theory predicts the peaks in the d^2I_c/dV_g^2 dependencies of the QDs corresponding to the quantum confined energy levels in the QDs[20]. Accordingly, the steps should be observed in the dI_c/dV_g spectra of the QDs as it has been observed in the BEEM spectra of the Au NCs in YSZ films in the present study (Fig. 4).

The BEEM/BHEM spectra of the nanocomposite YSZ:nc-Au/Si films were measured with reduced $I_t = 2$ nA (*i. e.* 5 times lower than in the pinhole measurements of the YSZ/Si

reference samples described in the previous subsection) and with the V_g sweep amplitude limited to 2.5 V just in order not to damage the YSZ:nc-Au film. Provided these precautions, the steps related to the quantum confined states in the Au NCc were well reproducible in the curves measures at both forward and backward V_g sweep. The absence of the hysteresis in the BEEM/BHEM spectra evidenced the non-destructive nature of the measurements in this mode.

The BHEM spectra of the Au(5 nm)/YSZ(3 nm)/nc-Au/YSZ(3 nm)/*n*-Si stack measured between the Au NCs (Fig. 4) exhibited the thresholds at $V_g = (2.6 \pm 0.1)$ V attributed to the YSZ valence band edge E_v, as in the reference Au/YSZ/Si sample (Fig. 1). The spectra measured on the Au NCs demonstrated the stepwise features similar to the ones observed in the BEEM spectra. These features were attributed to the ballistic electron tunnelling from the Si valence band states into the free states above Fermi level in the STM tip material via the quantum confined states in the Au NCs falling into the interval between $E_{v\mathrm{Si}}$ and E_v (see Fig. 2). This phenomenon could be also described in terms of the ballistic hole injection from the STM tip into the valence band states in the Si substrate via the quantum confined states in the Au NCs below E_F. Note that according to the BHES data, the bottom of the potential well of Au NCs in YSZ matrix $E_{c\mathrm{Au}} \approx -5.5$ eV appears to be lower than $E_v \approx -2.7$ eV. Thus, the Au QDs in the YSZ matrix appeared to be the ones of type II.

Using the data on the energy gaps in the Au/YSZ:nc-Au/*n*-Si(001) stacks provided by BEES/BHES (Fig. 2), the size quantization spectra for the electrons in the Au NCs have been calculated as a function of the NC diameter D_c according to the model of a spherical QD with a finite potential barrier height in the effective mass approximation[21]. The applicability of the latter for the structures studied in the present work was justified by the nanocrystallinity of the YSZ layers in the samples under study, as it has been already discussed above. Along with the standard boundary constraints for the continuity of the radial parts of the envelope wavefunctions of the bound electron states $\chi(r)$ at the YSZ/Au interface: $\chi_{\mathrm{Au}} = \chi_{\mathrm{YSZ}}$, Bastard's boundary constraints were imposed onto the envelope derivatives:

$$m_{\mathrm{Au}} \frac{\partial \chi_{\mathrm{Au}}}{\partial r} = m_{\mathrm{YSZ}} \frac{\partial \chi_{\mathrm{YSZ}}}{\partial r} \qquad (3)$$

where m_{Au} and m_{YSZ} are the effective electron masses in Au and YSZ, respectively. We assumed ($m_{\mathrm{YSZ}} = 0.7$)[22] and $m_{\mathrm{Au}} = 1$. The envelope wavefunction were considered to be twofold spin-degenerated, the spin-orbit interaction as well as Coulomb one for the electrons inside the QDs were neglected.

An example of the size quantization energy spectrum in an Au NC calculated for $D_c = 1.96$ nm is presented in Fig. 5. The value of $D_c = 1.96$ nm provided the best fit between the calculated quantum confined state energies in the NC and the experimental ones determined from the BEEM/BHEM spectra presented in Fig. 4.

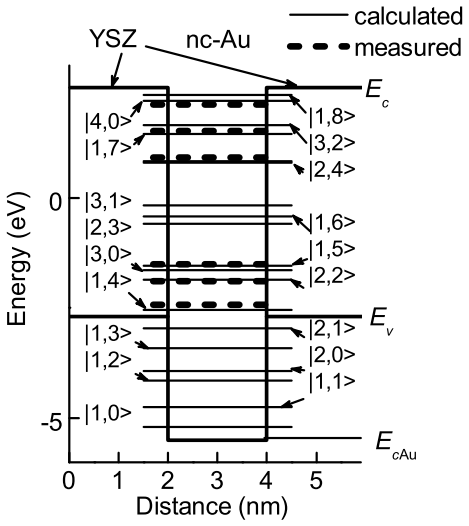

Fig. 5 A band diagram of an Au NC in YSZ matrix. The measured quantum confined state energies in the Au NC determined from the BEEM/BHEM spectra presented in Fig. 4 and the ones calculated according to a spherical QD model for the NC diameter $D_c = 1.96$ nm providing the best fit between the calculated and measured quantum confined level energies are shown. The quantum confined levels are marked as $|r,l\rangle$ where r and l are the radial and momentum squared quantum numbers, respectively.

The statistical analysis of the BEEM/BHEM spectra recorded in several spots of the increased I_c by the best fit between the calculated quantum confined states energies and the measured ones yielded an estimate of $D_c = 2.5 \pm 0.8$ nm. Taking into account that the effective mass approximation is a rather rough one for the Au NCs in YSZ matrix, the agreement of this estimate with the TEM data[19] could be considered to be satisfactory.

4 Conclusions

The results of present study demonstrate the capabilities of BEEM/BHEM in imaging the Au NCs inside the YSZ films and in measuring the size quantization energies of electrons in small enough Au NCs directly. As neither the apparatus used nor the experimental techniques developed were the material specific ones, one can expect BEEM/BHEM method to be applicable to the NCs made from any metal (or even from semiconductor, *e.g.* Si quantum dots in SiO_2 films, *etc*.) embedded into thin films of any dielectric (*e.g.* polymers, *etc*.) as well. So far, the present results indicate the prospects for

wide application of BEEM/BHEM for characterization of the ultrathin dielectric films with metal or semiconductor NCs in research and also in production.

5 Acknowledgements

The work was supported by Ministry of Education and Science, Russian Federation (State Research Program, Task 2014/134, Project 2591). The BEEM/BEES measurements were performed in Research and Educational Center for Physics of Solid State Nanostructures, Lobachevskii University of Nizhni Novgorod.

References

1 E. Coplin and U. Simon, *Metal Nanoclusters in Catalysis and Materials Science: the Issue of Size Control*, Elsevier, Amsterdam, 2008, p. 107.
2 V. P. Zhdanov and B. Kasemo, *Surf. Sci. Rep.*, 2000, **39**, 25–104.
3 V. P. Halperin, *Rev. Mod. Phys.*, 1986, **58**, 533–606.
4 C. Binns, *Surf. Sci. Rep.*, 2001, **44**, 1–49.
5 E. Bar-Sadeh, Y. Goldstein, C. Zhang, H. Deng, B. Abeles and O. Millo, *Phys. Rev. B*, 1994, **50**, 8961–8964.
6 H. Imamura, J. Chiba, S. Mitani and K. Takanashi, *Phys. Rev. B*, 2000, **61**, 46–49.
7 D. A. Antonov, D. O. Filatov, A. V. Zenkevich and Y. Y. Lebedinskii, *Bull. Russ. Acad. Sci., Phys.*, 2007, **71**, 56–59.
8 A. Zenkevich, Y. Lebedinskii, O. Gorshkov, D. Filatov and D. Antonov, *Advances in Diverse Industrial Applications of Nanocompositess*, InTech, Rijeka, 2011, pp. 317–340.
9 W. Guan, S. Long, R. Jia and M. Liu, *Appl. Phys. Lett.*, 2007, **91**, 062111+3.
10 V. Narayanamurti and M. Kozhevnikov, *Phys. Rep.*, 2001, **349**, 447–516.
11 M. A. Lapshina, M. A. Isakov, D. O. Filatov, S. V. Tikhonov, Y. A. Matveev and A. V. Zenkevich, *J. Surf. Investigation: X-ray, Synchrotron, and Neutron Techniques*, 2010, **4**, 411–418.
12 H. A. Abbas, *Stabilized Zirconia for Solid Oxide Fuel Cells or Oxygen Sensors. Characterization of Structural and Electrical Properties of Zirconia Doped with Some Oxides*, LAP Lambert Academic, 2012.
13 A. Bauer and R. Ludeke, *J. Vac. Sci. Technol. B*, 1994, **12**, 2667–2652.
14 K. Seeger, *Semiconductor Physics. An Introduction*, Springer, Berlin, 2004.
15 J. Robertson, *J. Vac. Sci. Techn. B*, 2000, **18**, 1785–1791.
16 D. Wilk, R. M. Wallace and J. M. Anthony, *J. Appl. Phys.*, 2001, **89**, 5243–5275.
17 G. Ozdemir and S. Maghsoodloo, *Smithells Metals Reference Book*, Elsevier, Amsterdam, 2004, p. 39.
18 S. Heiroth, R. Ghisleni, T. Lippert, J. Michler and A. Wokaun, *Acta Mater.*, 2011, **59**, 2330–2340.
19 S. V. Tikhov, O. N. Gorshkov, D. A. Pavlov, I. N. Antonov, A. I. Bobrov, A. P. Kasatkin, M. N. Koryazhkina and M. E. Shenina, *Tech. Phys. Lett.*, 2014, **40**, 369–371.
20 J. Walachova, J. Zelinka, V. Malina, J. Vanis, F. Sroubek, J. Pangrac, K. Melichar and E. Hulicius, *Appl. Phys. Lett.*, 2008, **92**, 012101+3.
21 A. Messiah, *Quantum Mechanics*, North Holland, Amsterdam, 1967, vol. 1, p. 78.
22 T. V. Perevalov, A. V. Shaposhnikov, K. A. Nazyrov, D. V. Gritsenko, V. A. Gritsenko and V. M. Taplin, *Defects in HIgh-k Gate Dielectric Stacks: Nano-Electronic Semiconductor Devices*, Springer, Berlin, 2006, p. 430.

Ballistic Electron Emission Microscopy was applied to imaging and spectroscopy of metal nanoclusters (NCs) in dielectric films. The possibility of measuring the size quantization energies in the NCs was demonstrated.